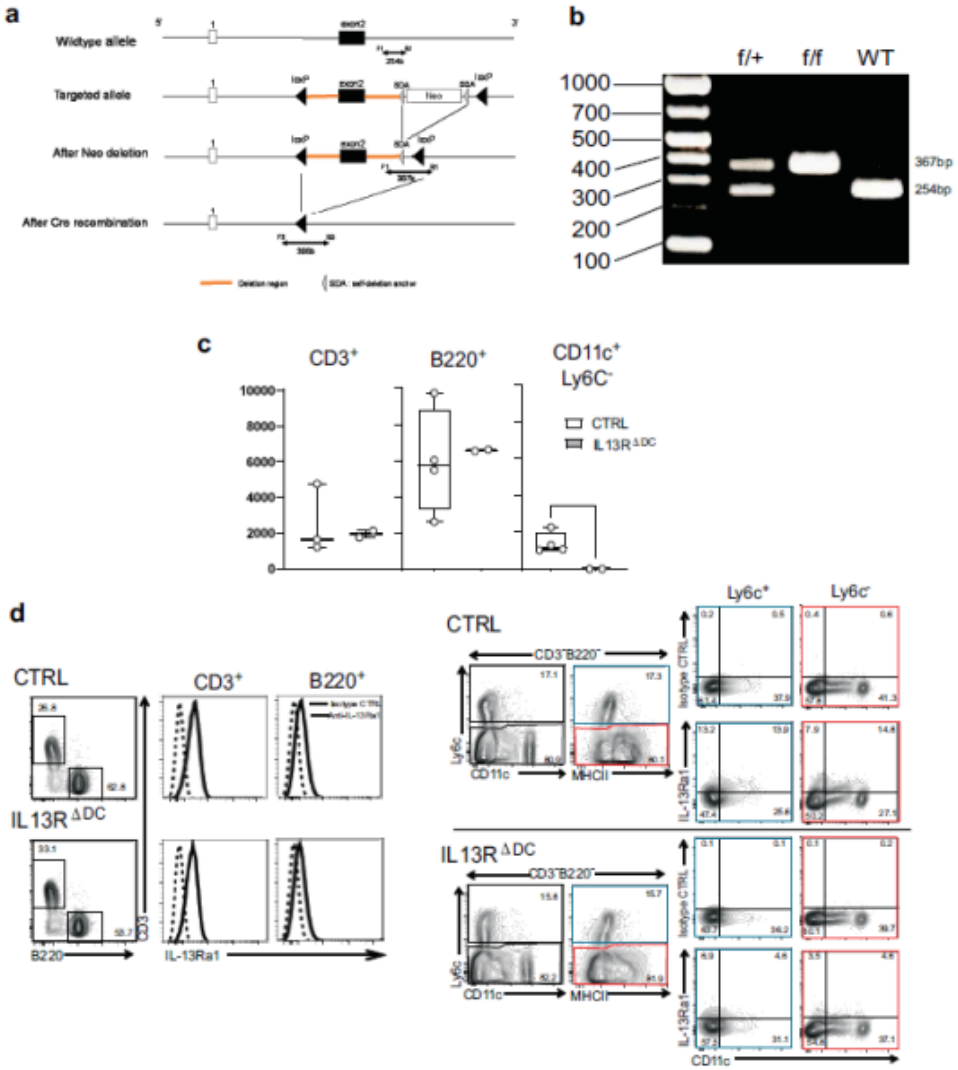

S-Figure 1. **Generation of *Il13ra1*$^{flox/flox}$ mice and DC-specific deletion in *Il13ra1*$^{flox/flox}$ mice by crossing with CD11c-cre mice (IL-13R$^{\Delta DC}$ mice).** (a) The strategy for targeting exon 2 of the *Il13ra1* gene. The Neo cassette was inserted at the 3' side of exon 2 (see "Targeted allele") and deleted by self-deletion (see "After neo deletion"). The bottom indicates the target allele after Cre-recombination. (b) Genotyping was performed by PCR (F1 and R1 primers). The flox (f) and wild-type (WT) alleles represent 367 bp and 254 bp, respectively. (c) *Il13ra1* gene expression in T cells (CD3$^+$), B cells (B220$^+$), and DCs (CD11c$^+$Ly6C$^-$) of IL13R$^{\Delta DC}$ mice. *Il13ra1* transcript levels were assessed by RT-PCR. The values indicate the copy number after normalized by *b-actin* copy number. (d) DC-specific deletion of cell surface expression of IL-13Rα1. Cells were obtained from the spleen of CTRL and IL-13R$^{\Delta DC}$ mice. The left panel shows IL-13Rα1 expression on T (CD3$^+$) and B (B220$^+$) cells. The right panel shows IL-13Rα1 expression on monocyte/macrophage (Ly6C$^+$) and DCs (CD11c$^+$ Ly6C$^-$) cells in the CD3$^-$ and B220$^-$ populations. Staining was performed using isotype control (mouse IgG1-biotin) or anti-IL-13Rα1(1G3 mouse IgG1-biotin) in combination with avidin-PE.

The data were representative of three independent experiments.

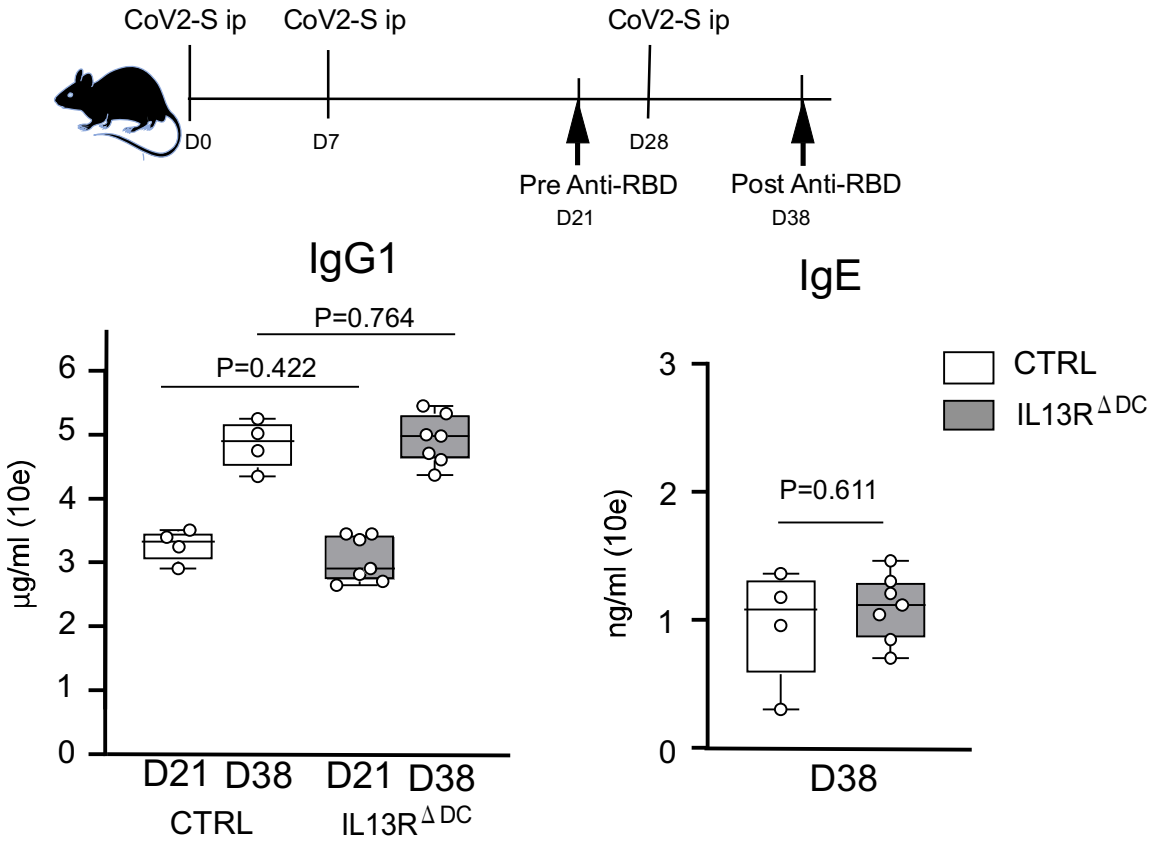

S-Figure 2. **Role of the IL-13 signal in systemic vaccination responses.** CTRL (n=4) and *Il13ra1*$^{\Delta DC}$ (n=7) mice were i.p. immunized with a recombinant trimer SARS-CoV-2 spike protein in alum adjuvant at D0, D7, and D28 (boosting). Anti-RBD IgG1 and IgE were measured by ELISA at D21 and D38.

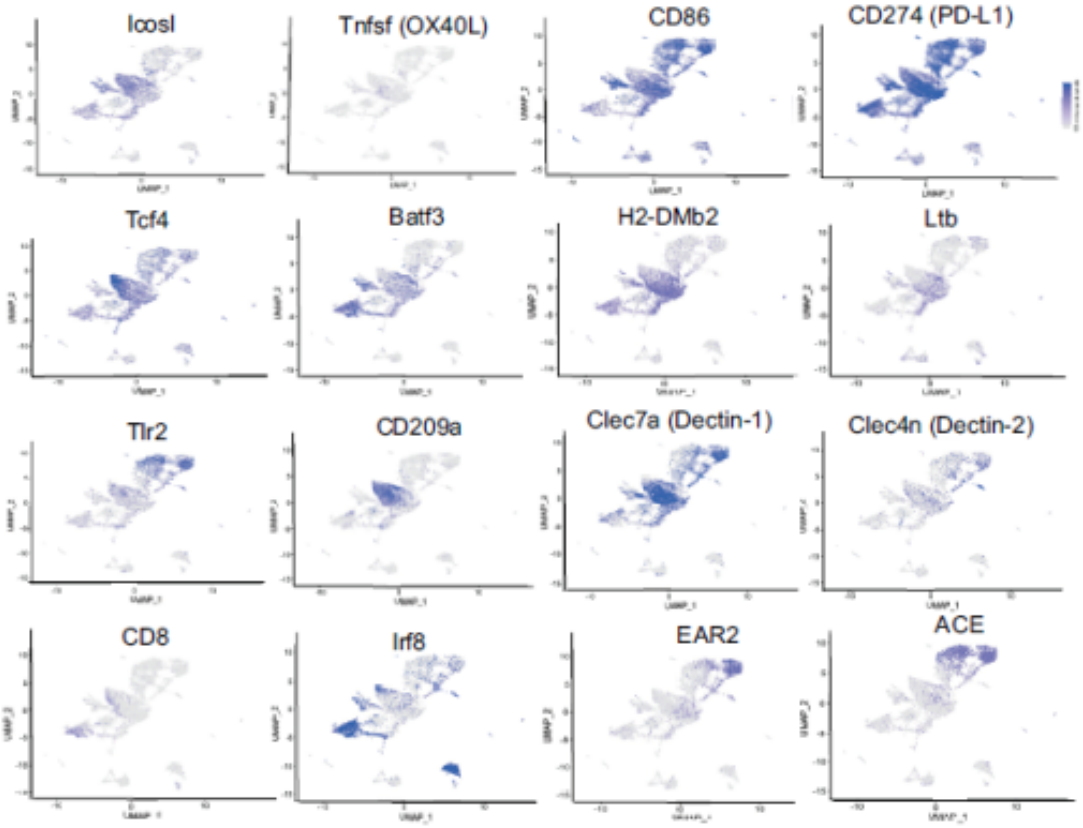

S-Figure 3. **Gene expression profiles of splenic CD11c^{+} cells.** The expression of cDC2 (Batf3), cDC1 (CD8 and Irf8), and monocyte/macrophage (EAR2 and ACE) markers and costimulation molecules by splenic CD11c^{+} cells from CAS+NP-OVA treated mice was analyzed by scRNAseq, as described in Figure 3a.

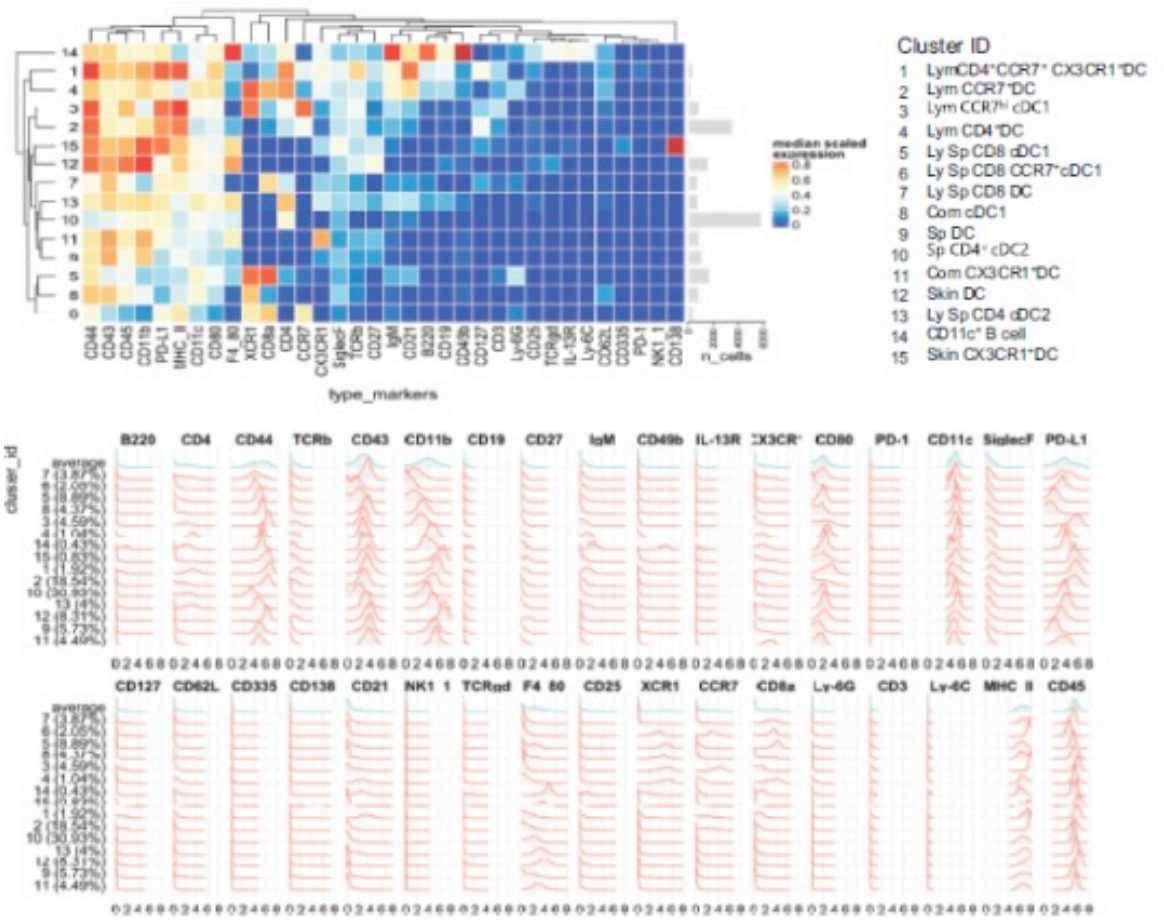

S-Figure 4. **Heatmap diagram and cytometric staining profile of 15 clusters in CyTOF analysis.** Cells were obtained from the skin, dLNs, and spleen of NS (n=3), CAS (n=3), and CAS+NP-OVA (n=3) mice and stained with the Maxpar OnDemand Mouse Immune Profiling Panel Kit. The upper panel shows the heatmap diagram of the $CD3^-$ $CD19^-$ $Ly6C^-$ $Ly6G^-$ $CD11c^+$ $MHCII^+$ cells in the NS, CAS, and CAS+NP-OVA treated mice. The lower panels show the cell surface expression of 34 molecules in the same populations, indicated by cluster ID on the left side.

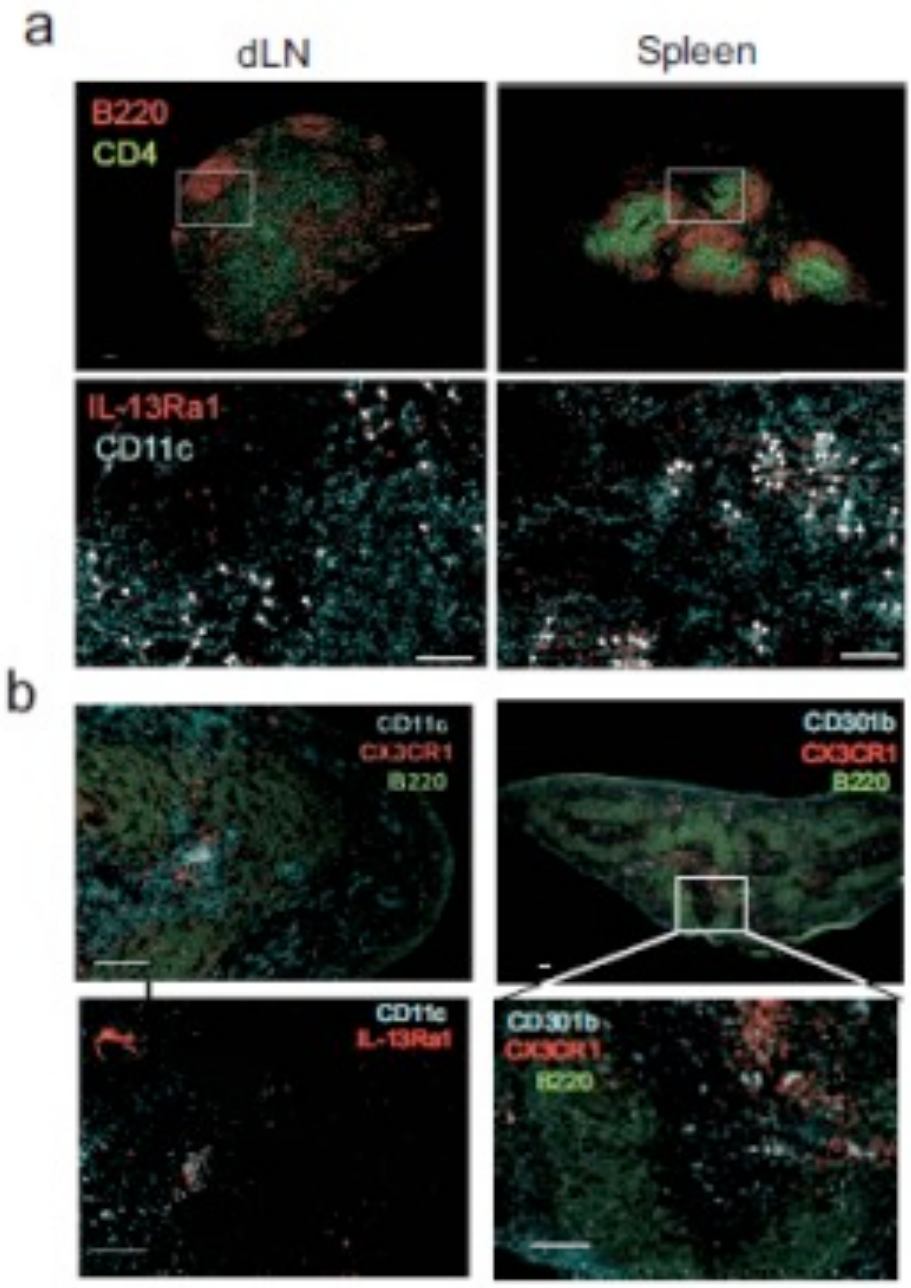

S-Figure 5. **Localization of IL-13R DCs at the T-B border.** (a) Localization of CD11c and IL-13Ra1 double-positive cells. The upper panel indicates the B220 (red) and CD4 (green) staining of the dLN after CAS (n=3) (left) and spleen after CAS+NP-OVA (n=3) (right) (X4). The lower panel shows the IL-13Ra1(red) and CD11c (blue) staining in the region surrounded by the white box in the upper panel (X20). The arrowheads indicate CD11c and IL-13Ra1 double-positive cells. (b) Localization of IL-13Ra1^{+}DCs overlapped with expression of CX3CR1 and CD301b. The two left panels show the CD11c/ CX3CR1/ B220 triple- and the CD11c/IL-13Ra1 double-staining in serial sections (X20). The right panel shows the CD301b/ CX3CR1/ B220 triple-staining: the upper shows X4, and the lower shows the area surrounded by the white box at X20.

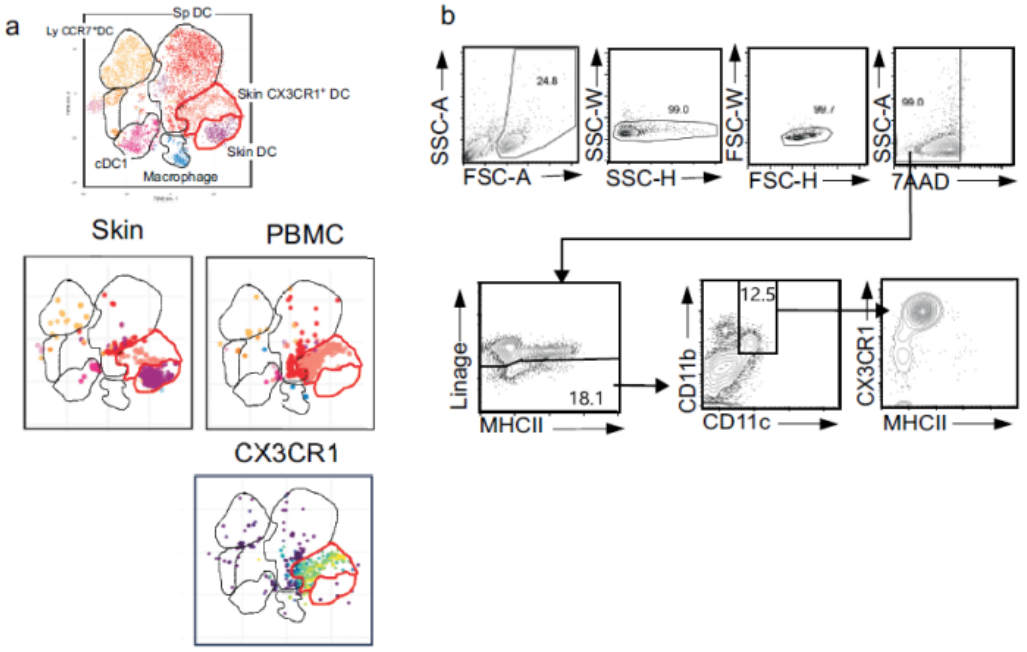

S-Figure 6. **CX3CR1^{+} DCs are abundant in PBMC** (a) CyTOF data from the CD3^{-} CD19^{-} CD11c^{+} MHCII^{+} cells: The upper panel shows the t-SNE algorithm of DC clusters in the mixture of CyTOF data obtained from skin, dLNs, spleen, and PBMC. The middle panel shows DC distribution in skin and PBMC. The lower panel shows the expression of CX3CR1. (b) Flow data: PBMC in unprimed mice stained with lin (CD3, B220), CX3CR1, MHCII, CD11b, and CD11c. The lower panel shows CD11c/CD11b and CX3CR1/MHCII in the Lin^{-} population.

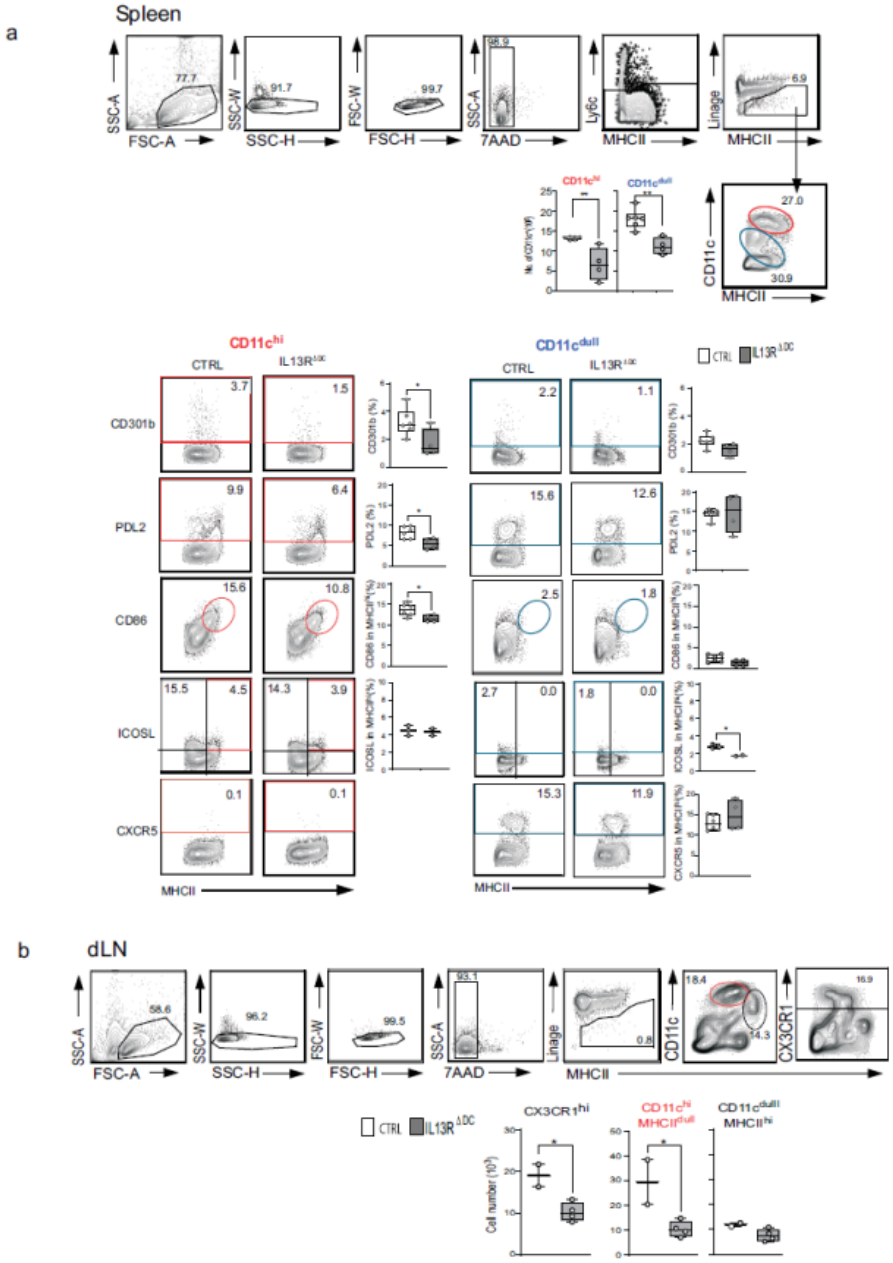

S-Figure 7 The impact of the IL-13 signal on CD11^{hi}DCs.
(a)The impact of the IL-13 signal in the inflamed spleen. The upper panel shows the gate settings for CD11c^{hi} and CD11c^{dull} population in the spleen obtained from CTRL (n=6) and *Il13ra1*$^{\Delta DC}$ (n=4) CAS+NP-OVA treated mice (D33). Cells were stained as described in Fig.4c, and the data shows cell numbers of CD11c^{hi} and CD11c^{dull} populations. The bottom left shows representative flow cytometry data of CTRL and Il13ra1$^{\Delta DC}$. The right panel shows the percentage of CD301b^{+}, CD86^{+}, PDL2^{+}, or ICOSL^{+} in the CD11c^{hi} and CD11c^{dull} populations.
(b) The impact of the IL-13 signal in the dLN. The upper panel shows the gate settings for CD11c^{hi} MHCII^{dull}, CD11c^{dull} MHCII^{hi}, and CX3CR1^{hi} populations in the dLNs obtained from CTRL (n=2) and Il13ra1ΔDC (n=4) CAS-treated mice (D19). The lower shows cell numbers of CX3CR1hi DC and CD11c^{hi} MHCII^{dull} or CD11c^{dull} MHCII^{hi} DCs.

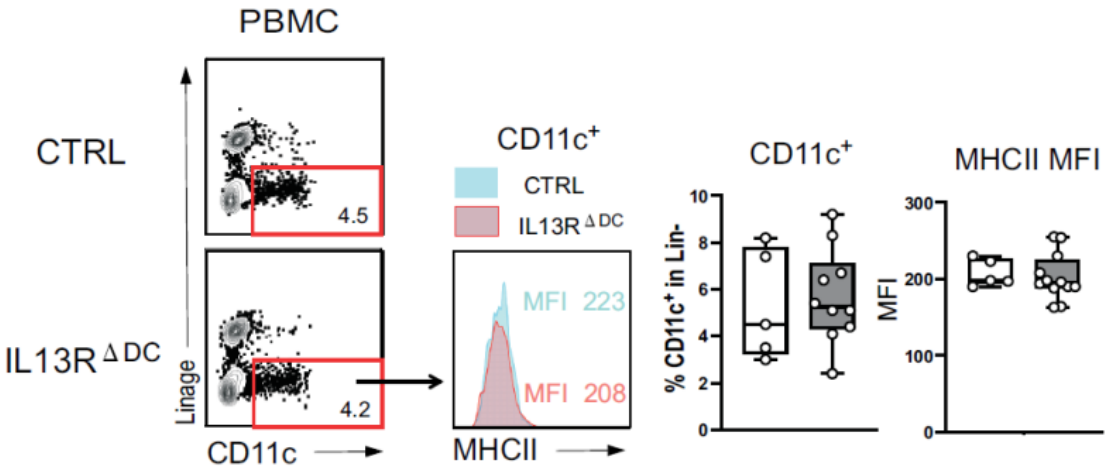

S-Figure 8 No impact of the IL-13 signal in MHCII expression of PMDC
The left panel shows the Lin$^-$ CD11c$^+$ populations gated and representative data for MHCII expression. The right shows the percentage of CD11c$^+$ cells in PBMC and the MHCII expression levels (MFI). CTRL (n=5) and *Il13ra1*$^{\Delta DC}$ (n=10) were used.

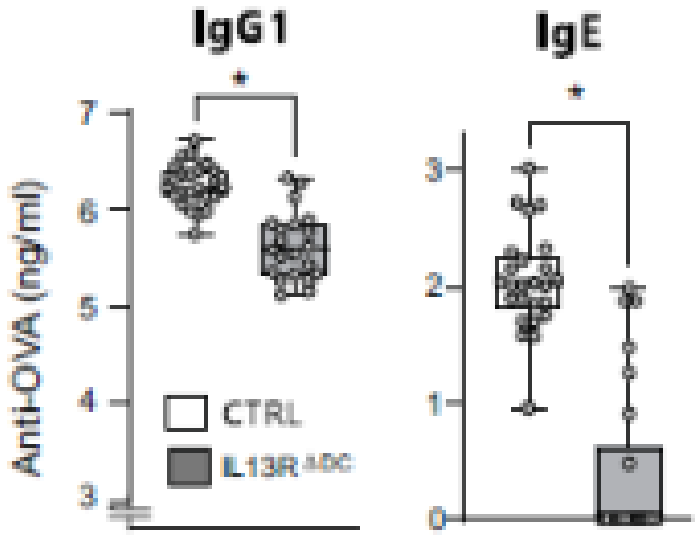

S-Figure 9 Anti-OVA IgG1 and IgE responses induced by CAS treatment.
CTRL (n=25) and *Il13ra1*$^{\Delta DC}$ (n=20) were treated with CAS (MC903+OVA) as described in Fig.1. IgG1 and IgE titers were measured at D19.

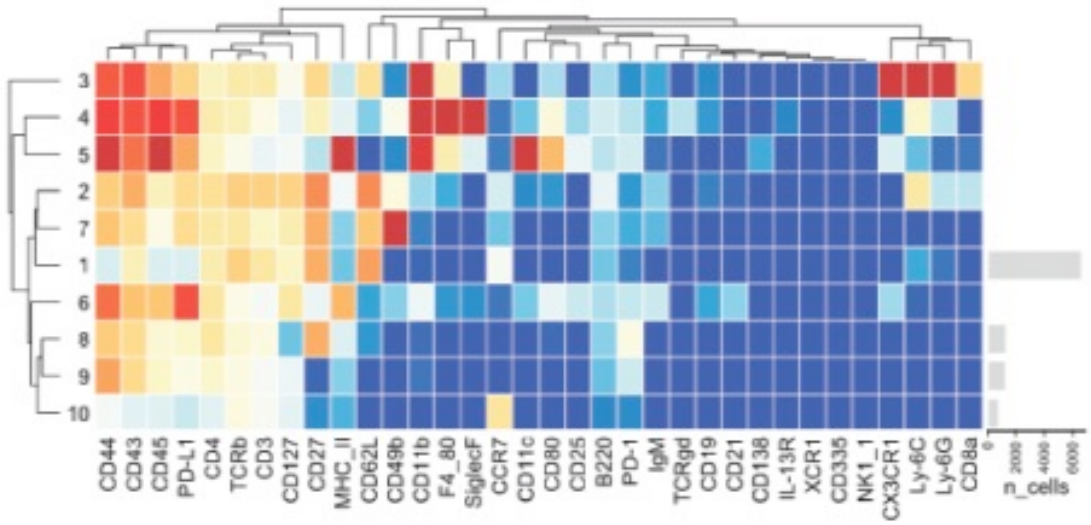

S-Figure 10 Heatmap diagram of 10 clusters in CyTOF analysis.
The CyTOF analysis was performed as described in Fig.6a. The data shows the heatmap diagram of the $CD3^{+}$ $CD19^{-}$ $TCRb^{+}$ $TCRgd^{-}$ $CD4^{+}$ $CD8^{-}$ cells in combined data of the NS (n=2), CAS (n=3), and CAS+NP-OVA (n=3) treated mice.

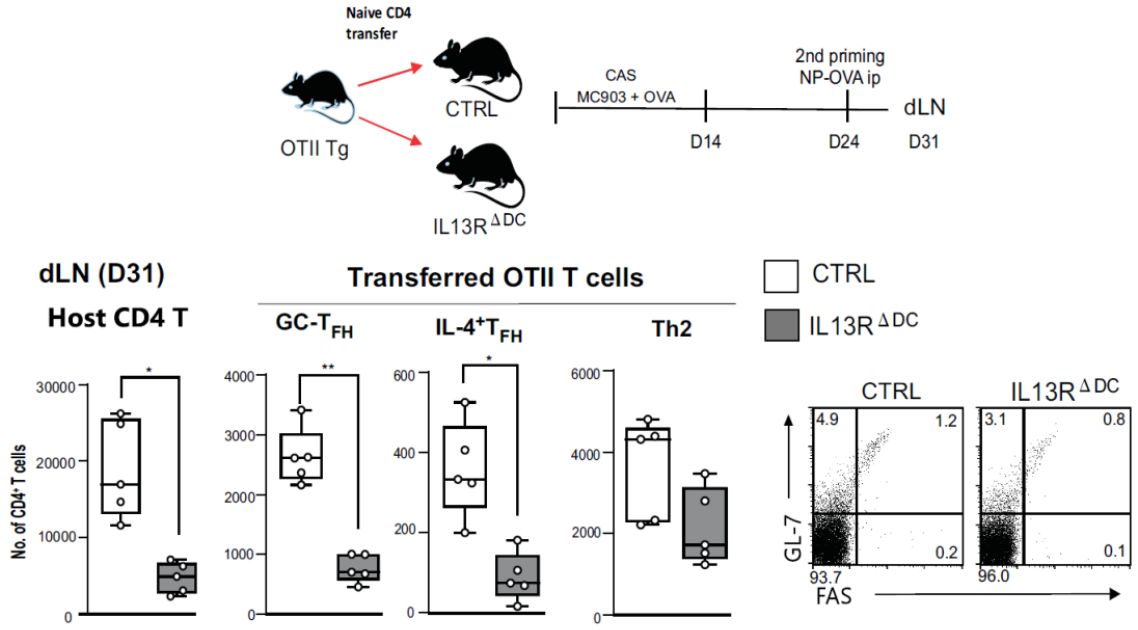

S-Figure 11

Development of Th2 and T_{FH} cells in the dLNs after systemic immunization. The dLN cells were obtained from CTRL (n=5) and IL-13RΔDC (n=5) mice. The figure shows host CD4 T cell and transferred OTII GC-T_{FH}, IL-4$^{+}T_{FH}$, and Th2 cell numbers in the dLN of the CAS+NP-OVA mice on D31. Data are shown as mean ± SD, unpaired *t*-test. P values are indicated as * p<0.05, ** p<0.01

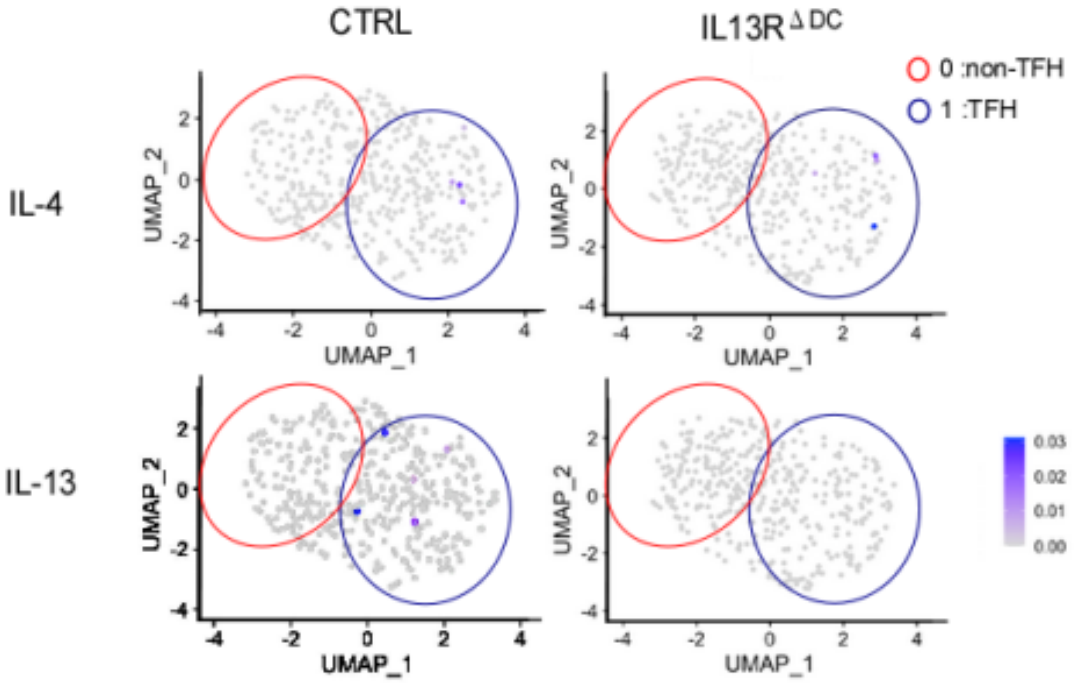

S-Figure 12. ***Il4* and *Il13* gene expression of the transferred OTII T cells in the control and IL-13R$^{\Delta DC}$ mice.** TCRVB5^{+} OTII T cells were sorted from the D31 spleen cells of the transferred mice described in **Fig. 6c** and scRNAseq analysis was performed. The red circle illustrates cluster 0, indicating non-T_{FH} gene expression. Dark blue illustrates cluster 1, indicating T_{FH} gene expression. The *Il4* and *Il13* expression profiles in clusters 0 and 1 of the CTRL and IL-13R$^{\Delta DC}$ mice are depicted by blue dots.

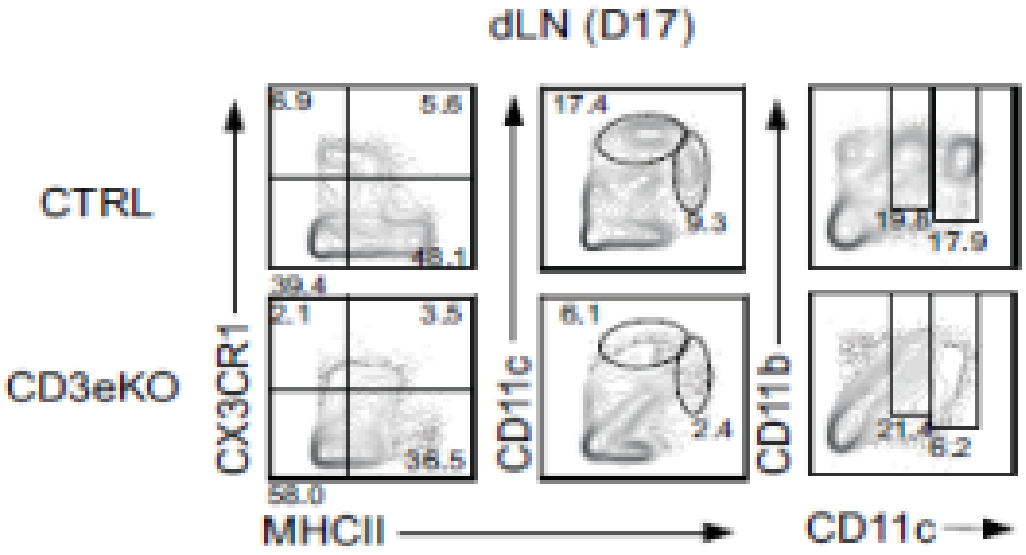

S-Figure 13. **Reduction of DC migration into the dLN of *Cd3e*-deficient mice.**
The dLNs were obtained from CTRL and CD3eKO CAS-treated mice (D17) as described in Fig.7a. The data are representative, showing $CD11c^{hi}$ $MHCII^{dull}$, $CD11c^{dull}$ $MHCII^{hi}$, and $CX3CR1^{hi}$ cells in the lin^- population.